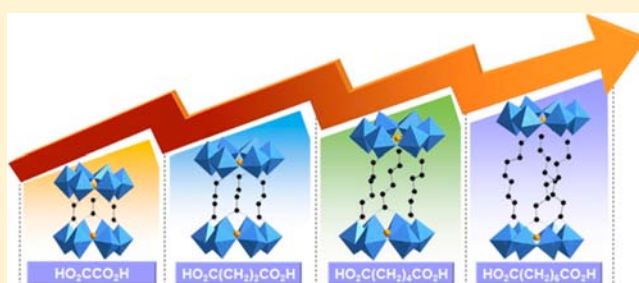


Controlled Assembly of Inorganic–Organic Frameworks Based on $[\text{SeMo}_6\text{O}_{21}]^{4-}$ PolyanionDonghui Yang,[†] Suzhi Li,[‡] Pengtao Ma,[†] Jingping Wang,^{*,†} and Jingyang Niu^{*,†}[†]Henan Key Laboratory of Polyoxometalate, Institute of Molecular and Crystal Engineering, College of Chemistry and Chemical Engineering, Henan University, Kaifeng, 475004 Henan, China[‡]College of Chemistry and Chemical Engineering, Engineering Research Center of Functional Material Preparation, Shangqiu Normal University, Shangqiu, 476000 Henan, China

Supporting Information

ABSTRACT: The chemical system based on $[\text{SeMo}_6\text{O}_{21}]^{4-}$ polyanion and carboxylate ligand has been investigated. According to the inherent nature of organic groups, a series of selenomolybdates with three architectures have been isolated through rational and deliberate synthetic routes by stereospecific addition of different carboxylic acids. Such an approach is potentially interesting for $\{\text{SeMo}_6\}$ cluster, which exhibits a high surface nucleophilicity and is capable of being functionalized by covalently bound carboxylic acids. Investigation of the assemblies reveals that carboxylic acids have good flexibility and conformational freedom, representing the powerful chemical tools to control the polyanion assembly processes.



INTRODUCTION

The assembly of inorganic–organic hybrid materials based on polyoxometalates (POMs) has gained increasing attention not only for extending their intriguing diverse architectures but also for exploring their potential applications in catalysis, medicine, biology, magnetism, and materials science.¹ The past decade has viewed the development of the POM-based covalently linked frameworks. Generally, Keggin,² Dawson,³ Anderson,⁴ and Lindqvist-type⁵ polyoxoanions are used as the inorganic building blocks to construct covalent hybrid materials.⁶ Among them, POMs templated by nonconventional (pyramidal or octahedral) heteroanions are much less developed.⁷ Moreover, the incorporation of pyramidal heteroanions with stereochemically active lone-pair electrons influences the assembly process, in which the lone-pair electron plays an important structure controlling role.^{7,8} As a matter of fact, we supposed that it would be of great interest to develop the syntheses of nonconventional polyoxomolybdate family bearing carboxylate function. So far, vast varieties of carboxylate-functionalized polyoxomolybdates have been synthesized and characterized spanning a great range of structural types. As for these complexes, the majority are isopolymolybdates, such as $\{\text{Mo}_2\text{O}_4\}^{2+}$,⁹ $\{\text{Mo}_8\text{O}_{28}\}^{4-}$,¹⁰ and $\{\text{Mo}_{2n}\text{O}_{2n}\text{S}_{2n}(\text{OH})\}_{2n}^{11}$ derivatives, and other isopolymolybdate anions bridged by RCOO^- groups or chelating carboxylate ligands.¹² In contrast, carboxylate-functionalized heteropolymolybdates are rarely known,^{7,13} and the linking of heteropolymolybdates with multicarboxylic acids have remained largely unexplored.^{13c} Nevertheless, there is also a major problem, for it is hard to control the assembly process to afford elaborate structures from

simple constituents. Indeed, the architectural design principles are almost empirical, mainly according to the intuition of the assembly processes and phenomena, which are drastically altered by temperature, pH, ionic strength concentration, etc. Judicious selection of appropriate linkers allows for a higher degree of predictability in geometric ordering.¹⁴ In the present study, we provide a target assembly by ligand control.

Herein, we have targeted the syntheses of modular functional nonconventional heteropolymolybdates with a well-established building block strategy. These compounds have further led to the development of the surface-grafted functionalized POMs. In particular, depending on inherently different natures and possible synergetic effects between the carboxylate ligands and POM clusters, these complementary components assemble to yield three different architectures (see Figure 1). In this work, we report the isolation of six new selenite-based carboxylate-functionalized polyoxomolybdates: $(\text{C}_3\text{N}_2\text{H}_5)_3\text{H}_2[\text{SeMo}_6\text{O}_{21}(\text{CH}_3\text{CO}_2)_3]\cdot 8\text{H}_2\text{O}$ (**1**), $(\text{NH}_4)_9\text{H}[(\text{SeMo}_6\text{O}_{21})_2(\text{C}_2\text{O}_4)_3]\cdot 10\text{H}_2\text{O}$ (**2**), $(\text{NH}_4)_{10}[(\text{SeMo}_6\text{O}_{21})_2\{\text{O}_2\text{C}(\text{CH}_2)_2\text{CO}_2\}_3]\cdot 15\text{H}_2\text{O}$ (**3**), $(\text{NH}_4)_{10}[(\text{SeMo}_6\text{O}_{21})_2\{\text{O}_2\text{C}(\text{CH}_2)_4\text{CO}_2\}_3]\cdot 8\text{H}_2\text{O}$ (**4**), $(\text{NH}_4)_{10}[(\text{SeMo}_6\text{O}_{21})_2\{\text{O}_2\text{C}(\text{CH}_2)_6\text{CO}_2\}_3]\cdot 10\text{H}_2\text{O}$ (**5**), and $(\text{NH}_4)_{32}[(\text{SeMo}_6\text{O}_{21})_6\{\text{C}_5\text{H}_3\text{N}(\text{CO}_2)_2\}_{10}]\cdot 26\text{H}_2\text{O}$ (**6**). Importantly, their dimension and composition can be stereochemically oriented and conformationally ordered by different carboxylic acids: acetic acid ($\text{CH}_3\text{CO}_2\text{H}$), oxalic acid ($\text{H}_2\text{C}_2\text{O}_4\cdot 2\text{H}_2\text{O}$), succinic acid ($\text{HO}_2\text{C}(\text{CH}_2)_2\text{CO}_2\text{H}$), adipic

Received: July 12, 2013

Published: December 3, 2013

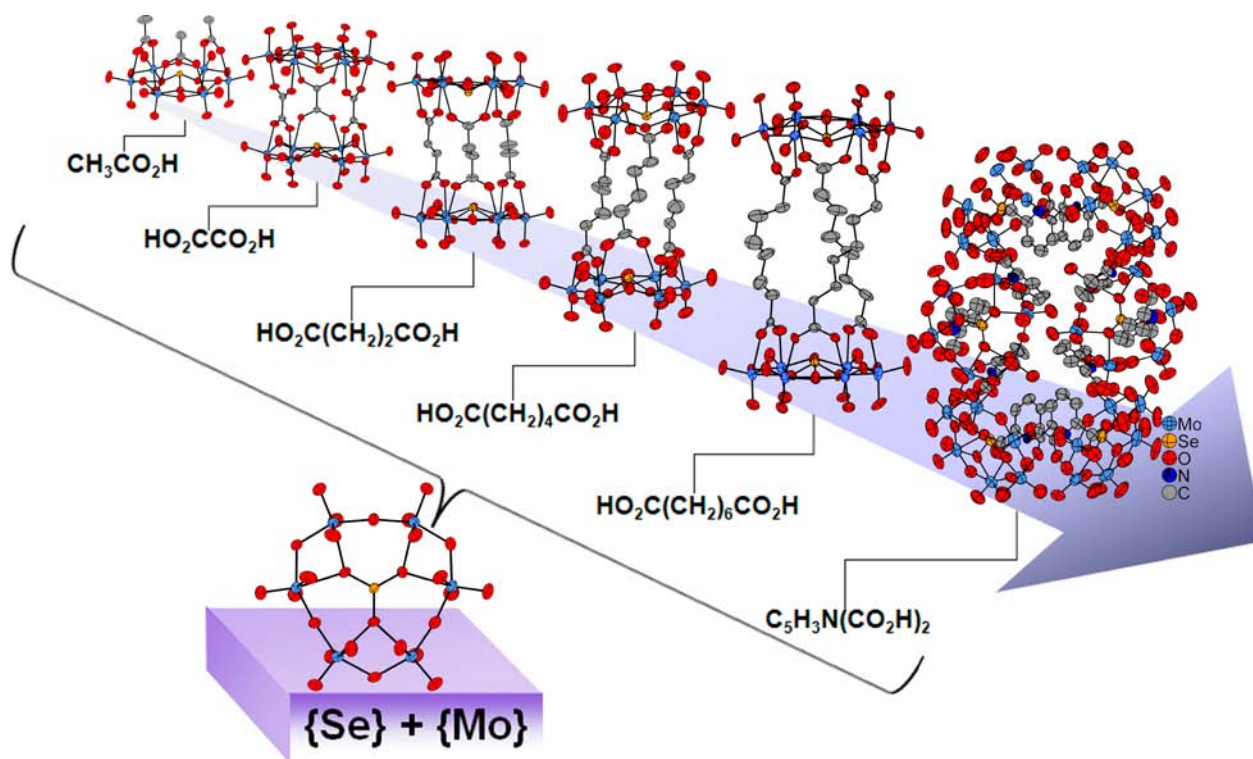


Figure 1. ORTEP drawings of the anion parts of 1–6 drawn at 50% probability level highlighting the assembly processes.

acid ($\text{HO}_2\text{C}(\text{CH}_2)_4\text{CO}_2\text{H}$), suberic acid ($\text{HO}_2\text{C}(\text{CH}_2)_6\text{CO}_2\text{H}$), and pyridine-2,6-dicarboxylic acid ($\text{C}_5\text{H}_3\text{N}(\text{CO}_2\text{H})_2$).

EXPERIMENTAL SECTION

Materials and Physical Measurements. All chemical reagents were purchased from commercial sources and used without further purification. IR spectra were recorded on a Bruker VERTEX 70 IR spectrometer using KBr pellets in the range of $4000\text{--}400\text{ cm}^{-1}$. C, H, and N elemental analyses were performed on a Perkin-Elmer 2400-II CHNS/O analyzer. Variable temperature powder X-ray diffraction (VT XRD) was performed from ambient temperature to 483 K on a Bruker AXS D8 Advance diffractometer using $\text{Cu K}\alpha$ radiation in the range $2\theta = 10\text{--}40^\circ$. EPR experiment of compound 5 was performed on a Bruker ER-2000-DSRC10 spectrometer at the X-band at 300 K after heating at 453 K for 7 h. UV–vis spectra were determined on a Shimadzu UV 3600 spectrophotometer.

Synthesis of 1. $\text{Na}_2\text{MoO}_4 \cdot 2\text{H}_2\text{O}$ (0.73 g, 3.02 mmol) and NaAc (0.25 g, 3.05 mmol) were dissolved in water (10 mL), then SeO_2 (0.05 g, 0.45 mmol) and imidazole (0.11 g, 1.62 mmol) were added. The pH of this mixture was adjusted to 4.7 by the addition of acetic acid, and the reaction mixture was heated at 70°C for 2 h, cooled, filtered, and left to evaporate slowly. Colorless block crystals of 1 appeared after about four weeks. Yield: 0.46 g (68%) for 1 based on SeO_2 . Elemental analysis calcd (%) for $\text{C}_{15}\text{H}_{42}\text{Mo}_6\text{N}_6\text{O}_{35}\text{Se}$ (1): C 11.84, H 2.78, N 5.52. Found: C 11.59, H 2.52, N 5.25. IR (KBr pellet): 3531(s), 3469(s), 3245(s), 3149(s), 2985(m), 2853(m), 1627(m), 1561(s), 1441(m), 1096(w), 1051(w), 934(s), 909(s), 786(s), 738(s), 663(s), 628(s), 504(m), 423 cm^{-1} (m).

Synthesis of 2. $(\text{NH}_4)_6\text{Mo}_7\text{O}_{24} \cdot 4\text{H}_2\text{O}$ (1.06 g, 0.86 mmol) was dissolved in water (15 mL), then SeO_2 (0.11 g, 0.99 mmol) and oxalic acid $\text{H}_2\text{C}_2\text{O}_4 \cdot 2\text{H}_2\text{O}$ (0.19 g, 1.51 mmol) were added. The reaction mixture was stirred approximately 2 h at 70°C to result in a colorless solution, cooled, filtered, and left to evaporate slowly. Colorless block crystals of 2 appeared after about four weeks. Yield: 0.60 g (47%) for 2 based on SeO_2 . Elemental analysis calcd (%) for $\text{C}_6\text{H}_7\text{Mo}_{12}\text{N}_9\text{O}_{64}\text{Se}_2$ (2): C 2.78, H 2.23, N 4.87. Found: C 3.17, H 3.10, N 4.74. IR (KBr

pellet): 3467(s), 3139(s), 1633(s), 1401(s), 1333(s), 934(s), 900(s), 779(s), 749(s), 670(s), 669(s), 529(m), 439 cm^{-1} (m).

Synthesis of 3. Same procedure as for 2, but 0.18 g (1.53 mmol) of succinic acid instead of oxalic acid. Yield: 0.74 g (54%) for 3 based on SeO_2 . Elemental analysis calcd (%) for $\text{C}_{12}\text{H}_{82}\text{Mo}_{12}\text{N}_{10}\text{O}_{69}\text{Se}_2$ (3): C 5.18, H 2.97, N 5.04. Found: C 5.24, H 3.03, N 4.95. IR (KBr pellet): 3449(s), 3158(s), 1626(m), 1558(s), 1403(s), 1234(w), 1161(w), 931(s), 898(s), 783(s), 737(s), 670(s), 512(m), 432 cm^{-1} (w).

Synthesis of 4. Same procedure as for 2, but 0.22 g (1.51 mmol) of adipic acid instead of oxalic acid, then added 0.15 g (2.80 mmol) of NH_4Cl . Yield: 0.58 g (43%) for 4 based on SeO_2 . Elemental analysis calcd (%) for $\text{C}_{18}\text{H}_{80}\text{Mo}_{12}\text{N}_{10}\text{O}_{62}\text{Se}_2$ (4): C 7.90, N 5.12. Found: C 7.61, H 3.17, N 4.87. IR (KBr pellet): 3469(s), 3167(s), 1627(m), 1554(s), 1408(s), 1336(m), 1215(w), 1146(w), 928(s), 896(s), 779(s), 739(s), 667(s), 511(m), 440 cm^{-1} (m).

Synthesis of 5. Same procedure as for 2, but 0.26 g (1.49 mmol) of suberic acid instead of oxalic acid. Yield: 0.55 g (39%) for 5 based on SeO_2 . Elemental analysis calcd (%) for $\text{C}_{24}\text{H}_{96}\text{Mo}_{12}\text{N}_{10}\text{O}_{64}\text{Se}_2$ (5): C 10.09, H 3.39, N 4.90. Found: C 9.68, H 3.46, N 4.85. IR (KBr pellet): 3450(s), 3164(s), 1624(m), 1549(s), 1406(s), 1306(w), 1099(w), 930(s), 901(s), 782(s), 737(s), 665(s), 513 cm^{-1} (m).

Synthesis of 6. Same procedure as for 2, but 0.25 g (1.50 mmol) of pyridine-2,6-dicarboxylic acid instead of oxalic acid, then added 0.15 g (2.80 mmol) of NH_4Cl . Yield: 0.34 g (24%) for 6 based on SeO_2 . Elemental analysis calcd (%) for $\text{C}_7\text{H}_{210}\text{Mo}_{36}\text{N}_{42}\text{O}_{192}\text{Se}_6$ (6): C 9.73, H 2.45, N 6.81. Found: C 9.92, H 3.18, N 6.62. IR (KBr pellet): 3436(s), 3165(s), 3034(s), 1606(s), 1570(s), 1398(s), 1273(w), 1081(w), 932(s), 903(s), 788(s), 739(s), 725(s), 664(s), 514 cm^{-1} (m).

RESULTS AND DISCUSSION

Synthesis. The covalent grafting of organic components onto POM clusters is an active field of research due to the diversity of chemical and physical properties. These attractive features have led to intense investigation of their synthetic strategy, and the advantage of covalent grafting in terms of

Table 1. Crystallographic Data for 1–6

	1	2	3
empirical formula	C ₁₅ H ₄₂ Mo ₆ N ₆ O ₃₅ Se	C ₆ H ₅₇ Mo ₁₂ N ₉ O ₆₄ Se ₂	C ₁₂ H ₈₂ Mo ₁₂ N ₁₀ O ₆₉ Se ₂
formula weight	1521.13	2588.81	2779.76
space group	P1	P $\bar{1}$	P $\bar{1}$
crystal system	triclinic	triclinic	triclinic
<i>a</i> (Å)	10.6278(6)	11.9029(4)	11.329(5)
<i>b</i> (Å)	10.6429(6)	13.8995(5)	16.310(8)
<i>c</i> (Å)	19.9819(12)	22.6008(8)	23.618(11)
α (deg)	76.2610(10)	96.0570(10)	86.496(9)
β (deg)	82.2280(10)	98.7630(10)	77.384(8)
γ (deg)	87.0640(10)	100.2130(10)	71.585(8)
<i>V</i> (Å ³)	2174.9(2)	3603.1(2)	4041(3)
<i>Z</i>	2	2	2
goodness-of-fit on <i>F</i> ²	1.033	1.039	1.016
<i>R</i> ₁ , <i>wR</i> ₂ [<i>I</i> > 2σ(<i>I</i>)]	0.0460, 0.1318	0.0355, 0.1001	0.0481, 0.1089
<i>R</i> ₁ , <i>wR</i> ₂ [all data]	0.0538, 0.1392	0.0474, 0.1059	0.0898, 0.1205
	4	5	6
empirical formula	C ₁₈ H ₈₀ Mo ₁₂ N ₁₀ O ₆₂ Se ₂	C ₂₄ H ₉₆ Mo ₁₂ N ₁₀ O ₆₄ Se ₂	C ₇₀ H ₂₁₀ Mo ₃₆ N ₄₂ O ₁₉₂ Se ₆
formula weight	2737.80	2858.31	8640.40
space group	P2(1)/ <i>n</i>	P2(1)/ <i>c</i>	P $\bar{1}$
crystal system	monoclinic	monoclinic	triclinic
<i>a</i> (Å)	18.3195(10)	24.247(6)	16.6345(16)
<i>b</i> (Å)	27.2576(15)	16.319(4)	22.046(2)
<i>c</i> (Å)	19.4976(11)	22.904(6)	22.650(4)
α (deg)	90	90	107.116(3)
β (deg)	114.5910(10)	114.664(5)	91.140(3)
γ (deg)	90	90	111.423(2)
<i>V</i> (Å ³)	8853.0(8)	8236(3)	7313.8(15)
<i>Z</i>	4	4	1
goodness-of-fit on <i>F</i> ²	1.080	1.001	1.011
<i>R</i> ₁ , <i>wR</i> ₂ [<i>I</i> > 2σ(<i>I</i>)]	0.0537, 0.1730	0.0667, 0.1232	0.0797, 0.1617
<i>R</i> ₁ , <i>wR</i> ₂ [all data]	0.0874, 0.1931	0.1670, 0.1455	0.2214, 0.1910

stability and structure control underlines the exceptionally great efforts in synthetic interest. However, it remains difficult to design or predict the relevant geometric relationships between the organic groups and POMs due to the little directional information. Studies of our group have shown that the assembly of {SeMo₆} cluster in aqueous solution can be controlled by grafting different carboxylic acid linkers. The key points of assembly processes have been well established, which indicate this synthetic approach supplying a feasible and controllable way for designing and making specific frameworks in the presence of carboxylic acids. It is noteworthy that the aliphatic dicarboxylic acid templates in 2–5 have the same orientation to give relevant insights about POM architectures. For example, the dimers were isolated when the dicarboxylic acids HO₂C-(CH₂)_{*n*}-CO₂H (*n* = 0, 2, 4, 6) acted as the linkers. Interestingly, the inclusion of dicarboxylic species within POM-based frameworks reveals an attractive general pattern. The dimeric motifs are formed with two carboxyl groups at the same sides of the zigzag carbon chain; however, larger polymer would be obtained with two carboxyl groups at different sides of the carbon chain (see Figure S1 in the Supporting Information).

Structure of the Anions. One-pot syntheses of 1–6 have been achieved by the reactions of NaMoO₄·2H₂O or (NH₄)₆Mo₇O₂₄·4H₂O, SeO₂ and corresponding carboxylate ligands in a weakly acidic aqueous solution for 2 h. A summary of crystallographic data and structural refinements for 1–6 is given in Table 1. It is interesting to find they possess the similar chemical and structural information, and their degree of

polymerization is synthetically controlled by the carboxylic acids. The six compounds contain the common {SeMo₆} unit. The representation of {SeMo₆} cluster is shown in Figure S2, Supporting Information. The cluster consists of six MoO₆ octahedra, forming a ring by alternate edge- and corner-sharing. The selenate subunit shares three oxo-groups with the ring and the central Se atom is located slightly above the plane of molybdate ring, which presents a trigonal-pyramidal coordination geometry. X-ray analyses reveal that the bond lengths of Mo–O_t and Mo–O_b are close to these of the amino acids functionalized species.⁷ The flat arrangement of {SeMo₆} unit is similar to those single-side organically functionalized Anderson-type POMs.^{4b} Unlike Anderson-type POM units separated by alcoholates, the {SeMo₆} units in 1–6 are covalently connected via the carboxyl groups of carboxylate ligands.

The ball-stick and polyhedron representation of [(SeMo₆O₂₁)(CH₃CO₂)₃]³⁻ (1a) is shown in Figure 2. Structure of 1a exhibits a monomer arrangement, where covalent interactions between the {SeMo₆} unit and the carboxylate linkers result in a single mode of connections. This is similar to that previously observed in the amino acid-functionalized species.⁷ Likewise, each carboxyl group is coordinated to two edge-sharing Mo atoms in the symmetric bidentate coordination mode. As a result, three acetic acid ligands are bound to {SeMo₆} cluster on the same side of the molybdate ring. Further, the center Se atom, on which the lone pair of electrons is located, is orientated in the same direction

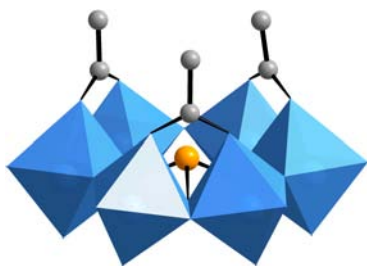


Figure 2. Ball-stick and polyhedron representation of $[(\text{SeMo}_6\text{O}_{21})(\text{CH}_3\text{CO}_2)_3]^{3-}$. Color code: MoO_6 (blue), Se (orange), and C (gray).

with acetic acid ligands. Consequently, $\{\text{COO}\}$ groups are orientated almost perpendicular to the $\{\text{SeMo}_6\}$ plane.

It is proven by the structure of **1** that using carboxylate ligands to functionalize heteropolymolybdates is feasible. Therefore, it may be predicted that there is the possibility of functionalization with dicarboxylate ligands to prepare dimers. This approach resulted in four novel molecular capsules **2–5**. The formation of these hybrid capsules can be envisaged by two $\{\text{SeMo}_6\}$ clusters linking intramolecularly by three dicarboxylate ligands. Three dicarboxylate linkers act as pillars within the scaffold structures of **2–5**. Both $\{\text{SeMo}_6\}$ units arrange in a face-to-face mode, appearing nearly superimposed. Thus, the anion $[(\text{SeMo}_6\text{O}_{21})_2(\text{C}_2\text{O}_4)_3]^{10-}$ (**2a**) can be properly described with the idealized D_{3h} symmetry (see Figure 3a). However, compounds **3–5** exhibit the unsymmetric superimposed structures owing to the flexibility of dicarboxylate linkers, arising from the distort of carbon chains (see Figure 3b,c,d). From these geometrical observations, dicarboxylate

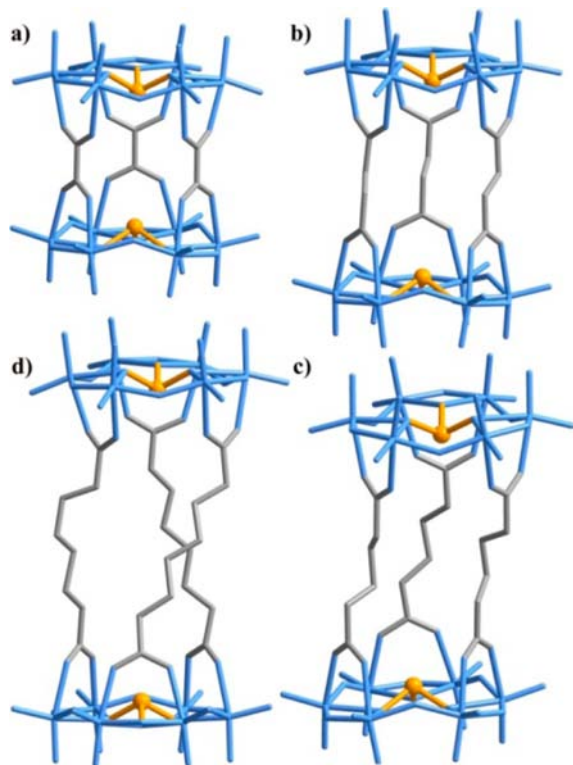


Figure 3. Structural representation of the anion **2–5** (a–d) highlighting the coordination of the carboxylate linkers. Color code: blue sticks = $\{\text{Mo}_6\}$ subunits; gray sticks = carboxylate linkers; Se = orange spheres.

ligands can be considered as flexible hinges, which allow the concerted screwed torsion to coordinate with $\{\text{SeMo}_6\}$ unit. It is worth noting that during our experimental exploration, the length of target structure could precisely be controlled by selecting appropriate dicarboxylate linkers.

The accessibility of **2–5** prompted us to use an other kind of dicarboxylate ligand exploiting the structural motif for the preparation of hybrid materials. Functionalization with rigid ligands can allow POM clusters to prepare porous networks,¹⁵ and thus, an aromatic ligand has been recognized and used in the design and construction of carboxylate derivatives.^{14a,16} The structural differences between aliphatic and aromatic dicarboxylic acids are evident. The asymmetric polyanion of **6** can be visualized as six $\{\text{SeMo}_6\}$ units linked by ten $\{\text{C}_5\text{H}_3\text{N}(\text{CO}_2)_2\}$ groups. As shown in Figure 4, each $\{\text{SeMo}_6\}$ unit acts as a

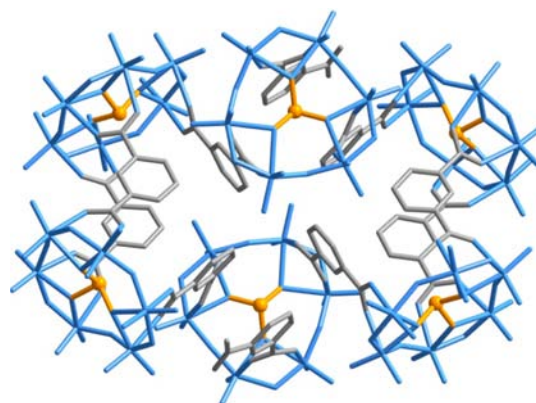


Figure 4. Structural representation of **6** highlighting the coordination of the carboxylate linkers. All cations and solvent water molecules are omitted for clarity. Color code: blue sticks = $\{\text{Mo}_6\}$ subunits; gray sticks = carboxylate linkers, Se = orange spheres.

tridentate ligand coordinating to three $\{\text{C}_5\text{H}_3\text{N}(\text{CO}_2)_2\}$ groups via the carbonyl oxygen of pyridine-2,6-dicarboxylic acid ligand to generate the hexasupported structure. Nevertheless, the striking feature for **6** lies in its pronounced structure transformation because the hexameric cluster appears strongly distorted to harmonize the change. In such an arrangement, six $\{\text{SeMo}_6\}$ units adopt a distinctly staggered conformation to cohere with pyridine-2,6-dicarboxylic acid and are mainly governed by steric constraints, resulting in the uncoordinated carboxyl groups of pyridine-2,6-dicarboxylic acids.

FT-IR Spectroscopy. IR spectra were used to investigate the structural characters of compounds **1–6** (see Figure S3 in the Supporting Information). Six compounds display similar characteristic patterns of the polyanion $[\text{SeMo}_6\text{O}_{21}]^{4-}$. The characteristic peaks at strong absorption bands in the range of $934\text{--}896\text{ cm}^{-1}$ are assigned to the vibrations of terminal $\text{Mo}=\text{O}$ units, and those in the range of $788\text{--}628\text{ cm}^{-1}$ are assigned to the vibrations of $\text{Mo}-\text{O}-\text{Mo}$ groups, leading to an overlap with the $\nu(\text{Se}-\text{O})$ stretching vibration bands.¹⁷ More specifically, the $\nu(\text{C}=\text{O})$ bands appear in the region $1633\text{--}1398\text{ cm}^{-1}$, which demonstrate the grafting of organic ligands onto the surface of POMs and are in good agreement with the results of single-crystal X-ray structural analyses. Compared to the uncoordinated carboxylic acid ($1700\text{--}1740\text{ cm}^{-1}$), the ν_{COO} vibrations of **1–6** are shifted to low frequency due to the interaction between carboxylate and metal ion.^{9a} The bands at $3531\text{--}3034\text{ cm}^{-1}$ with strong strength are probably a result of the stretching vibrations $\nu(\text{H}-\text{O})$ and $\nu(\text{N}-\text{H})$.

Variable Temperature IR Spectra and XRD. The solid-state thermostability of the aforementioned compounds has been investigated in ambient conditions by variable temperature IR spectroscopy and XRD. All the powder materials of 1–6 show a white coloration in their ground state. It is found that the heating of powders 1–6 induced obvious color changes, and the colors gradually shifted to dark-blue with a high coloration contrast. After heating of compounds 1–4 and 6 at 453 K in air for 0.5 h, the skeletal vibrations in the region between 450 and 1650 cm^{-1} were maintained (see Figure S4 in the Supporting Information), whereas they showed clear changes in the region between 450 and 1000 cm^{-1} at 483 K (see Figure S5 in the Supporting Information), indicating that the frameworks were at least partially decomposed at this temperature. However, the VT powder XRD data (see Figure S6 in the Supporting Information) shows that the dehydration initially results in the change of crystal lattice at 323 K, suggesting some changes occurred in the crystal structure. By comparison, 5 shows a fast coloration change, and its skeletal vibrations have changed at 453 K, while the main vibrations have little change until the temperature of 513 K (see Figure S7 in the Supporting Information).

EPR and UV–Vis Spectra. The dark blue powders 2–5 are soluble in water after heating at 453 K, and the color of sample solutions is deep blue. Nevertheless, powders 1 and 6 are difficult to dissolve in water at the same temperature. The color changes may be due to the reduction of the POMs. The formation of reduced metallic centers in 5 can be well evidenced by the EPR spectrum (see Figure S8 in the Supporting Information). The distinct paramagnetic signals with $g_1 = 1.917$ and $g_2 = 2.007$ can be attributed to Mo^{5+} .¹⁸ The deviation of the g values from g_e might be due to differences of Mo coordination environment.¹⁹ It is supposed that the intramolecular electron transfer between the organic groups and the POM moieties might result in the thermochromic behavior of these compounds. The electronic effect of 5 was observed in the UV–vis spectra. The diffuse reflectance spectrum of heated solid of 5 at 453 K for 7 h is shown in Figure S9 (see the Supporting Information) that shows the appearance of a broad feature at 340 nm. Here, the vast majority of dark blue powder can be dissolved in water. The UV–vis spectrum of blue solution 5 in the range of 200–800 nm is similar to the solution of ground state, which both reveal one characteristic peak (see Figure S10 in the Supporting Information), attributing to $p\pi-d\pi$ charge-transfer transition of the $\text{O}_t \rightarrow \text{Mo}$ bond. The blue solution changes into colorless solution gradually in the air for about 10 h, but the spectrum of the stored solution does not vary with time (see Figure S11 in the Supporting Information). The relative peak position of this heated powder in the solution state is different from its solid state UV–vis spectrum, which may suggest the different existential state in solution and the solid.

CONCLUSIONS

In summary, an efficient synthetic strategy to modify the nonconventional POM structures is potentially interesting for the formation of relevant deliberate architectures. Such simple chemical systems, based on the structural complementarities between $\{\text{Mo}_6\}$ reactive moieties and carboxylic acids, have led to the syntheses of a series of relevant clusters with target geometries. Furthermore, the assembly process appears to be highly versatile and sensitive to the nature of the carboxylate ligands, which represents the powerful templated role to

develop diverse POM-based systems. This work has important perspectives for controlling the directed assembly of covalent architectures. The syntheses of these compounds show that a great deal of structural design is possible in the covalently functionalized POM assemblies. In future work, we will investigate the ligand-mediated conformational switching via stereospecific addition of the carboxylic acids, as well as exploiting the incorporation of other heteroatoms.

ASSOCIATED CONTENT

Supporting Information

Thermogravimetric analyses of 1–6, and Figures S1–S12. This material is available free of charge via the Internet at <http://pubs.acs.org>.

AUTHOR INFORMATION

Corresponding Authors

*(J.W.) E-mail: jpwang@henu.edu.cn.

*(J.N.) E-mail: jyniu@henu.edu.cn.

Notes

The authors declare no competing financial interest.

ACKNOWLEDGMENTS

We thank the National Natural Science Foundation of China, the Foundation of Education Department of Henan Province, and Natural Science Foundation of Henan Province for financial support.

REFERENCES

- (1) (a) Gouzerh, P.; Proust, A. *Chem. Rev.* **1998**, *98*, 77–111. (b) Rhule, J. T.; Hill, C. L.; Judd, D. A. *Chem. Rev.* **1998**, *98*, 327–357. (c) Pope, M. T.; Müller, A. *Angew. Chem.* **1991**, *103*, 56–70; *Angew. Chem., Int. Ed.* **1991**, *30*, 34–48. (d) Proust, A.; Thouvenot, R.; Gouzerh, P. *Chem. Commun.* **2008**, 1837–1852. (e) Dolbecq, A.; Dumas, E.; Mayer, C. R.; Mialane, P. *Chem. Rev.* **2010**, *110*, 6009–6048.
- (2) (a) Joo, N.; Renaudineau, S.; Delapierre, G.; Bidan, G.; Chamoreau, L.-M.; Thouvenot, R.; Gouzerh, P.; Proust, A. *Chem.—Eur. J.* **2010**, *16*, 5043–5051. (b) Matt, B.; Renaudineau, S.; Chamoreau, L.-M.; Afonso, C.; Izzet, G.; Proust, A. *J. Org. Chem.* **2011**, *76*, 3107–3112.
- (3) (a) Pradeep, C. P.; Misrahi, M. F.; Li, F. Y.; Zhang, J.; Xu, L.; Long, D. L.; Liu, T. B.; Cronin, L. *Angew. Chem., Int. Ed.* **2009**, *48*, 8309–8313. (b) Nomiyama, K.; Togashi, Y.; Kasahara, Y.; Aoki, S.; Seki, H.; Noguchi, M.; Yoshida, S. *Inorg. Chem.* **2011**, *50*, 9606–9619.
- (4) (a) Favette, S.; Hasenknopf, B.; Vaissermann, J.; Gouzerh, P.; Roux, C. *Chem. Commun.* **2003**, 2664–2665. (b) Wu, P. F. P.; Yin, C.; Zhang, J.; Hao, J.; Xiao, Z. C.; Wei, Y. G. *Chem.—Eur. J.* **2011**, *17*, 12002–12005.
- (5) (a) Aronica, C.; Chastanet, G.; Zueva, E.; Borshch, S. A.; Clemente-Juan, J. M.; Luneau, D. *J. Am. Chem. Soc.* **2008**, *130*, 2365–2371. (b) Xia, Y.; Wei, Y. G.; Wang, Y.; Guo, H. Y. *Inorg. Chem.* **2005**, *44*, 9823–9828.
- (6) (a) Miras, H. N.; Yan, J.; Long, D. L.; Cronin, L. *Chem. Soc. Rev.* **2012**, *41*, 7403–7430. (b) Müller, A.; Gouzerh, P. *Chem. Soc. Rev.* **2012**, *41*, 7431–7463. (c) Banerjee, A.; Bassil, B. S.; Rösenthaler, G.-V.; Kortz, U. *Chem. Soc. Rev.* **2012**, *41*, 7590–7604. (d) Proust, A.; Matt, B.; Villanneau, R.; Guillemot, G.; Gouzerh, P.; Izzet, G. *Chem. Soc. Rev.* **2012**, *41*, 7605–7622.
- (7) Kortz, U.; Savelieff, M. G.; Ghali, F. Y. A.; Khalil, L. M.; Maalouf, S. A.; Sinno, D. I. *Angew. Chem., Int. Ed.* **2002**, *41*, 4070–4073.
- (8) (a) Corella-Ochoa, M. N.; Miras, H. N.; Kidd, A.; Long, D. L.; Cronin, L. *Chem. Commun.* **2011**, 47, 8799–8801. (b) Gao, J.; Yan, J.; Beeg, S.; Long, D. L.; Cronin, L. *Angew. Chem., Int. Ed.* **2012**, *51*, 1–5.
- (9) (a) Modéc, B.; Dolenc, D.; Kasunič, M. *Inorg. Chem.* **2008**, *47*, 3625–3633. (b) Modéc, B.; Brenčić, J. V.; Dolenc, D.; Zubieta, J.

Dalton Trans. **2002**, 4582–4586. (c) Modéc, B.; Dolenc, D.; Brenčič, J. V.; Koller, J.; Zubieta, J. *Eur. J. Inorg. Chem.* **2005**, 3224–3237. (d) Modéc, B.; Brenčič, J. V.; Burkholder, E. M.; Zubieta, J. *Dalton Trans.* **2003**, 4618–4625.

(10) (a) Liu, G.; Zhang, S. W.; Tang, Y. Q. *Z. Anorg. Allg. Chem.* **2001**, 627, 1077–1080. (b) Inoue, M.; Yamase, T. *Bull. Chem. Soc. Jpn.* **1995**, 68, 3055–3063. (c) Cartuyvels, E.; Van Hecke, K.; Van Meervelt, L.; Görrler-Walrand, C.; Parac-Vogt, T. N. *J. Inorg. Biochem.* **2008**, 102, 1589–1598. (d) Cindrić, M.; Novak, T. K.; Kraljević, S.; Kralj, M.; Kamenar, B. *Inorg. Chim. Acta* **2006**, 359, 1673–1680.

(11) (a) Salignac, B.; Riedel, S.; Dolbecq, A.; Sécheresse, F.; Cadot, E. *J. Am. Chem. Soc.* **2000**, 122, 10381–10389. (b) Cadot, E.; Sécheresse, F. *Chem. Commun.* **2002**, 2189–2197. (c) Lemonnier, J.-F.; Floquet, S.; Marrot, J.; Terazzi, E.; Pigué, C.; Lesot, P.; Pinto, A.; Cadot, E. *Chem.—Eur. J.* **2007**, 13, 3548–3557. (d) Lemonnier, J.-F.; Kachmar, A.; Floquet, S.; Marrot, J.; Rohmer, M.-M.; Bénard, M.; Cadot, E. *Dalton Trans.* **2008**, 4565–4574.

(12) (a) Yang, W. B.; Lu, C. Z.; Lin, X.; Zhuang, H. H. *Inorg. Chem.* **2002**, 41, 452–454. (b) du Peloux, C.; Mialane, P.; Dolbecq, A.; Marrot, J.; Sécheresse, F. *Angew. Chem., Int. Ed.* **2002**, 41, 2808–2810. (c) Zhou, Z. H.; Hou, S. Y.; Cao, Z. X.; Tsai, K. R.; Chow, Y. L. *Inorg. Chem.* **2006**, 45, 8447–8451. (d) Liu, G.; Zhang, S. W.; Tang, Y. Q. *J. Chem. Soc., Dalton Trans.* **2002**, 2036–2039. (e) Gao, G. G.; Xu, L.; Qu, X. S.; Liu, H.; Yang, Y. Y. *Inorg. Chem.* **2008**, 47, 3402–3407.

(13) (a) Kortz, U.; Vaissermann, J.; Thouvenot, R.; Gouzerh, P. *Inorg. Chem.* **2003**, 42, 1135–1139. (b) Cindrić, M.; Strukan, N.; Devčić, M.; Kamenar, B. *Inorg. Chem. Commun.* **1999**, 2, 558–560. (c) Yang, D. H.; Li, S. Z.; Ma, P. T.; Wang, J. P.; Niu, J. Y. *Inorg. Chem.* **2013**, 52, 8987–8992.

(14) (a) Zheng, S. T.; Zhang, J.; Yang, G. Y. *Angew. Chem., Int. Ed.* **2008**, 47, 3909–3913. (b) Hirano, T.; Uehara, K.; Uchida, S.; Hibino, M.; Kamata, K.; Mizuno, N. *Inorg. Chem.* **2013**, 52, 2662–2670. (c) Marrot, J.; Pilette, M. A.; Haouas, M.; Floquet, S.; Taulelle, F.; López, X.; Poblet, J. M.; Cadot, E. *J. Am. Chem. Soc.* **2012**, 134, 1724–1737.

(15) Breen, J. M.; Schmitt, W. *Angew. Chem., Int. Ed.* **2008**, 47, 6904–6908.

(16) Zheng, S. T.; Zhang, J.; Li, X. X.; Fang, W. H.; Yang, G. Y. *J. Am. Chem. Soc.* **2010**, 132, 15102–15103.

(17) Kong, F.; Hu, C. L.; Xu, X.; Zhou, T. H.; Mao, J. G. *Dalton Trans.* **2012**, 41, 5687–5695.

(18) (a) Baffert, C.; Boas, J. F.; Bond, A. M.; Kçgerler, P.; Long, D. L.; Pilbrow, J. R.; Cronin, L. *Chem.—Eur. J.* **2006**, 12, 8472–8483. (b) Kozieł, M.; Podgajny, R.; Kania, R.; Lebris, R.; Mathonière, C.; Lewiński, K.; Kruczala, K.; Rams, M.; Labrugère, C.; Bousseksou, A.; Sieklucka, B. *Inorg. Chem.* **2010**, 49, 2765–2772.

(19) Ng, V. W. L.; White, J. M.; Young, C. G. *J. Am. Chem. Soc.* **2013**, 135, 7106–7109.